

Development for Prediction Model for Environmental Condition of Deterioration Phenomena for Asset Integrity Management

Tetsuo Fuchino^{a,*}, Teiji Kitajima^b, Yukiyasu Shimada^c, Masazumi Miyazawa^d

^a Tokyo Institute of Technology, 2-12-1 O-okayama, Meguro, Tokyo, Japan

^b Tokyo University of Agriculture and Technology, 2-24-16 Naka-cho, Koganei-shi, Tokyo, Japan

^c National Institute of Occupational Safety and Health, Japan, 1-4-6, Umezono, Kiyose, Tokyo Japan

^d Best Materia Corporation, 2-43-15, Misawa, Hino-shi, Tokyo, Japan

fuchino@chemeng.titech.ac.jp

The occurrence and progress of a deterioration phenomenon in a chemical plant is determined by the construction material, the plant physical structure and the physical and chemical environmental condition. In order to ensure and maintain the reliability of the facility during operation, the environmental condition such as the concentration of the deterioration substances at the deterioration site should be managed. In this study, we propose an approach to develop a prediction model for physical and chemical environmental condition of deterioration phenomena consistent with the plant operation. The prediction model is composed of the three layers; the process information management layer, the process bulk simulation layer, and the microscopic environmental condition prediction layer. By integrating abovementioned three layers based on the observability and measurable nature of the interfacial variables, it becomes possible to synthesize multi-scale simulation-based environment to predict the environmental condition of deterioration phenomena.

1. Introduction

In these days, once a serious incident occurs, it may affect the sustainability of the business, so it is required to ensure and maintain the reliability of facilities in the chemical industry. The reliability of a facility is influenced by the deteriorations accompanying the operation. In order to ensure and maintain the reliability of the facility, the physical and chemical environmental condition such as the concentration of the deterioration substances at the deterioration site is to be managed. The environmental condition has been monitored by a limited number of sampling, so far. Originally, monitoring the environmental condition by sampling is an observation method for trend management on the assumption that the process operating condition does not change greatly. However, the operation is often forced to be changed greatly according to the market situation under the today's mega competitive situation. Thus, the sampling-based condition monitoring up to now is insufficient to manage asset integrity under today's change environment.

To overcome the above-mentioned problem, the prediction model for physical and chemical environmental condition of deterioration phenomena consistent with the plant operation is indispensable. In general, a deterioration phenomenon of a chemical plant occurs in a microscopic region, and the chemical and physical environmental condition is behaved within such a microscopic region. This microscopic behaviour is governed by the overall bulk fluid condition of the corresponding deteriorated equipment module and the bulk fluid condition are dominated by the process overall operation. Therefore, the prediction model for physical and chemical environmental condition should be composed of the three layers; the process information management layer correcting and providing the operation data, the process bulk simulation layer estimating the unmeasurable bulk fluid conditions in the corresponding equipment module from the operating data, and the microscopic environmental condition prediction layer. In this study, the phenomena leading to microscopic corrosion environmental conditions and their causal events are expressed as hierarchical causal relationships. By integrating abovementioned three layers based on the observability and measurable nature of these causal

events, it becomes possible to synthesize multi-scale environment to predict the environmental condition of deterioration phenomena.

2. Example of NH_4HS Corrosion in HDS process

In this study, development of an environmental condition prediction model is considered by using a case study of the ammonium bisulfide (NH_4HS) corrosion in the hydrodesulphurization (HDS) process.

2.1 HDS Process

Figure 1 shows a block flow diagram of the HDS process, which represents the HDS plant providing the operation data, here. The diesel fraction containing nitrogen and sulphur components from the battery limit is fed through the “D-201: Feed Surge Drum” and pressurized by the “P-201A/B: Feed Pump”. After mixed with hydrogen, it is preheated by the E-201, E-203: Reactor Feed/Effluent Exchangers” and further heated up to the predetermined temperature by the “H-201: Reactor Charge Heater”. In the “R-201: Reactor”, the sulphur hydrodesulphurization reaction (e.g.; $\text{RS-R} + \text{H}_2 = 2\text{R} + \text{H}_2\text{S}(\text{g})$), nitrogen hydro-denitrogenation reaction (e.g.; $\text{R}'\text{N} = \text{R}' + 3/2\text{H}_2 = \text{R} + \text{R}' + \text{NH}_3(\text{g})$) and decomposition reactions occur. The reactor effluent containing H_2S and NH_3 equivalent to sulphur and nitrogen in the “Feed Diesel Fraction” is heat recovered by the “E-203, E-201: Reactor Feed/Effluent Exchangers” and “E-202: Stripper Reboiler”, and furthermore is cooled to about 40 C in “C-204: Reactor Effluent Condenser (Air Fin Cooler)”. In the low temperature section of “C-204”, $\text{H}_2\text{S}(\text{g})$ and $\text{NH}_3(\text{g})$ react to form $\text{NH}_4\text{SH}(\text{s})$, which can cause under-deposit corrosion and blockage. To prevent forming of $\text{NH}_4\text{SH}(\text{s})$, sour condensate is injected at inlet of “C-204” to decreasing partial pressure of $\text{H}_2\text{S}(\text{g})$ and $\text{NH}_3(\text{g})$. this blockage, the reactor effluent is quenched before sent to the “C-204” by using vaporization heat of injection water. The sufficiently cooled reactor effluent is sent to the “D-202: High Pressure Separator”. In the “D-202”, a vapour containing H_2S and H_2 , an oil, and an aqueous phase are separated. The oil is further decompressed, and vapour liquid is separated by the “D-203: Low Pressure Separator”, and then purified by the “T-202: Stripper”. The gas containing H_2S and H_2 is sent to T-201 Amine Scrubber” to separate H_2S , and the remaining gas is recycled after being partially purged.

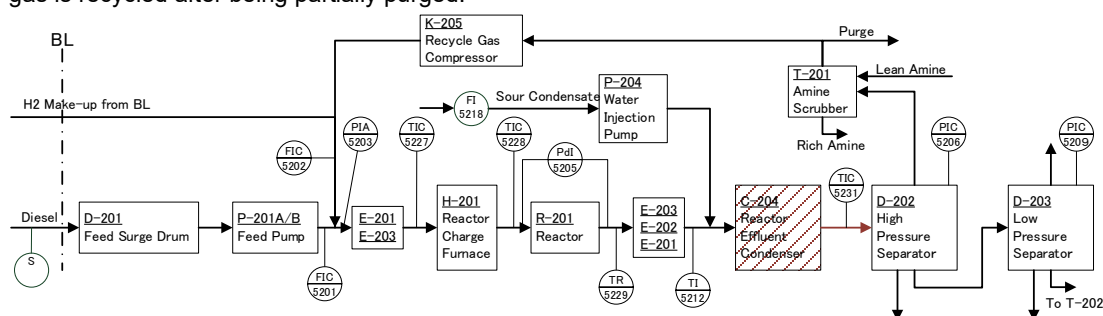


Figure 1: Block flow diagram of hydro desulphurization process.

2.2 NH_4HS Corrosion

The reactor effluent is supplied to the “C-204” at around 160C near the dew point of water by the latent heat of vaporization of injected water on the “C-204” inlet line, and cooled to about 40C by air. With cooling, the amount of condensate of light hydrocarbons and water in the vapor phase increases. Hydrocarbons in the diesel fraction and water are immiscible, and $\text{NH}_3(\text{g})$ and $\text{H}_2\text{S}(\text{g})$ are dissolved in the aqueous phase. The dissolved $\text{NH}_3(\text{aq})$ and $\text{H}_2\text{S}(\text{aq})$ form $\text{NH}_4\text{HS}(\text{aq})$, and it is known that NH_4HS corrosion is caused by $\text{NH}_4\text{HS}(\text{aq})$ dissolved in the aqueous phase, and that if its equivalent concentration in aqueous phase exceeds 35wt% (Scherrer et al. (1980)), severe corrosion will occur. Therefore, it is important to monitor or predict the weight concentration of NH_4HS in an aqueous phase as a corrosive environment, in order to ensure and maintain the reliability of facilities. In this study, we focus on the NH_4HS corrosion environment of C-204 tube.

The amount of NH_4HS dissolved in the aqueous phase increases with the amount of water condensed, and the NH_4HS corrosive environment becomes more severe as the outlet of “C-204” is approached. Near the outlet of “C-204”, considerable amounts of light hydrocarbons and water in the vapor phase are condensed. For this reason, it is expected that the volume velocity of the fluid falls and becomes a laminar flow region, and the vapor phase and the liquid phase flow separately in the tube. In such a case, the upper surface of the tube on the vapor phase side has a lower film heat transfer coefficient, and the tube surface temperature becomes substantially equal to the air temperature. Figure 2 shows an image of the flow inside the tube near the outlet of “C-204”. The water component of the tube vapor phase is under vapor pressure at the process bulk temperature

T_{Bulk} K. On the other hand, when the tube surface temperature T_{Surface} K reaches air temperature T_{Air} K ($< T_{\text{Bulk}}$ K), water droplets or film-like condensation occurs on the tube surface. Near the outlet of “C-204”, NH_4HS is absorbed by process bulk condensate and tube surface condensate. Therefore, as the corrosive environment, it is necessary to predict the NH_4HS concentration in these two aqueous phases at the same site.

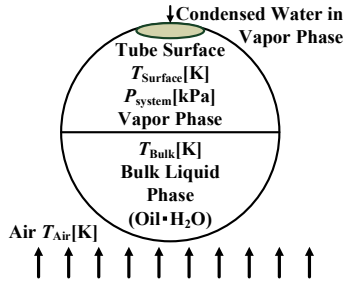


Figure 2 An image of the flow inside the tube

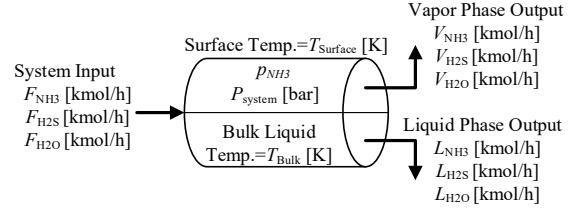


Figure 3 $\text{NH}_3\text{-H}_2\text{S-H}_2\text{O}$ system outline

3. Dissolution Model of NH_4HS in Aqueous Phase

In recent years, there have been many reports of the use of thermodynamic simulators using electrolyte properties to predict the corrosive environment (Toba 2013). NH_4HS corrosion is caused by NH_4HS dissolved in the aqueous phase as in other corrosive environments. Therefore, in order to accurately estimate the corrosion environment, the use of electrolyte properties is desired. However, utilization of electrolyte properties requires input of pH and electric potential. The NH_4HS corrosion target site in this study is inside the “Air Fin Cooler Tube”, and it is difficult to measure the pH and the electric potential of the surface condensate on the tube even if it is dissolved in the process bulk condensate.

In order to estimate the corrosive environment, the dissolution process of NH_4HS in the aqueous phase is not a major problem. In other words, there is no significant difference between estimating the dissolution equilibrium with an electrochemical equilibrium model nor with the overall equilibrium solubility model. It is said that hydrogen sulphide hardly dissolves in water, but it dissolves in an aqueous ammonia solution to form an apparent ammonium bisulfide ($\text{NH}_4\text{SH}(\text{aq})$) aqua. Assuming that this dissolution of H_2S in the aqueous ammonia solution is a neutralization reaction, it can be interpreted that H_2S equivalent to the ammonia dissolved in the aqueous phase at the maximum is dissolved in the aqueous phase to become an NH_4HS aqueous solution. The general style guidelines are first given, followed by specific cases. First of all, avoid lower-level heading immediately following the higher-level one. It is recommended to have at least one sentence in-between.

3.1 Ammonia Solubility Model

Sherwood (1925) published data on the solubility of ammonia in water, for each temperature. This data shows the partial pressure of ammonia in vapor phase and the mole fraction of liquid phase ammonia at different temperatures, and a solubility model of ammonia in aqua can be expressed by estimating the parameters of the general equilibrium equation as shown in Eq. (1). Where $x_{\text{NH}_3}^{\text{aq}}$ is ammonia mole fraction in aqua, T_{Bulk} is bulk fluid temperature and p_{NH_3} is ammonia partial pressure.

$$x_{\text{NH}_3}^{\text{aq}} = \exp\left(\frac{2061}{T_{\text{Bulk}}} - 10.279\right) \cdot p_{\text{NH}_3}^{0.5} - \exp\left(\frac{5556.6}{T_{\text{Bulk}}} - 26.793\right) \cdot p_{\text{NH}_3} \quad (1)$$

3.2 Dissolution Model in Bulk Condensed Aqueous Phase

As described with reference to Figure 2, the NH_4HS corrosion occurs at the tube metal regions contacting with the bulk condensed water and with the tube upper surface condensed water. In this section, a prediction model for the NH_4HS mass concentration in bulk aqueous condensate in the $\text{NH}_3\text{-H}_2\text{S-H}_2\text{O}$ system as shown in Figure 3 is considered. When r_{DSNH_3} ; ammonia dissolved fraction to the input NH_3 flow rate (F_{NH_3}), and $r_{\text{CDH}_2\text{O}}$; water condensate fraction to the input H_2O flow rate ($F_{\text{H}_2\text{O}}$) are set as internal variables, then the material balance equations between the input component molar flow rates and vapour/liquid phase output component molar flow rates as shown in Eqs. (2) to (4) are obtained.

$$V_{\text{NH}_3} = F_{\text{NH}_3} \cdot (1 - r_{\text{DSNH}_3}) \quad (2) \quad V_{\text{H}_2\text{S}} = F_{\text{H}_2\text{S}} - F_{\text{NH}_3} \cdot r_{\text{DSNH}_3} \quad (3)$$

$$V_{\text{H}_2\text{S}} = F_{\text{H}_2\text{S}} - F_{\text{NH}_3} \cdot r_{\text{DSNH}_3} \quad (4)$$

Furthermore, Eqs. (5) to (7) show the material balance equations between the input component molar flow rates and liquid phase output component molar flow rates.

$$L_{\text{H}_2\text{S}} = F_{\text{NH}_3} \cdot r_{\text{DSNH}_3} \quad (5) \quad L_{\text{H}_2\text{S}} = F_{\text{NH}_3} \cdot r_{\text{DSNH}_3} \quad (6)$$

$$L_{\text{H}_2\text{S}} = F_{\text{NH}_3} \cdot r_{\text{DSNH}_3} L_{\text{H}_2\text{O}} = F_{\text{H}_2\text{O}} \cdot r_{\text{CDH}_2\text{O}} \quad (7)$$

The total vapor and liquid flow rates (V_{system} and L_{system}) of this system can be described as shown in Eq. (8) and (9). The component molar fractions of vapor (y_{comp}) and liquid (x_{comp}) phases for each component can be described as shown in Eqs. (10) and (11), where the subscript comp indicates the composition element of NH_3 , H_2S and H_2O .

$$V_{\text{system}} = V_{\text{NH}_3} + V_{\text{H}_2\text{S}} + V_{\text{H}_2\text{O}} \quad (8) \quad L_{\text{system}} = L_{\text{NH}_3} + L_{\text{H}_2\text{S}} + L_{\text{H}_2\text{O}} \quad (9)$$

$$y_{\text{comp}} = V_{\text{comp}}/V_{\text{system}} \quad (10) \quad x_{\text{comp}} = L_{\text{comp}}/L_{\text{system}} \quad (11)$$

The partial pressure (p_{comp} bar) of each component is described as shown in Eq. (12) based on the material balance. The vapor pressure of water is a function of the temperature of the field and can be expressed with Eq. (13) by applying the modified Antoine's equation, where $p_{\text{H}_2\text{O}}^{\text{v}}$ is vapor pressure of water in bar.

$$p_{\text{comp}} = P_{\text{system}} \cdot V_{\text{comp}}/V_{\text{system}} \quad (12)$$

$$\ln(p_{\text{H}_2\text{O}}^{\text{v}}) = 61.323 - 7.2275 \times 10^3/T_{\text{Bulk}} - 7.177 \ln(T_{\text{Bulk}}) + 4.0313 \times 10^{-6} T_{\text{Bulk}}^2 \quad (13)$$

In this system, if a sufficient low pressure and an ideal solution could be assumed, then the molar fraction of water in the vapor phase ($y_{\text{H}_2\text{O}}^{\text{calc}}$) as shown in Eq. (14) can be obtained by applying Raoult's law.

$$y_{\text{H}_2\text{O}}^{\text{calc}} = p_{\text{H}_2\text{O}}^{\text{v}}/P_{\text{system}} \cdot x_{\text{H}_2\text{O}} \quad (14)$$

The internal variables $r_{\text{CDH}_2\text{O}}$ and r_{DSNH_3} are to be searched iteratively within a region of zero to one so that Eqs. (15) and (16) are sufficiently equal to zero to make consistent the material balance calculations shown in Eqs. (2) through (12) with the equilibrium calculations shown in Eqs. (1), (13), and (14).

$$|y_{\text{H}_2\text{O}} - y_{\text{H}_2\text{O}}^{\text{calc}}| \leq \varepsilon \quad (15) \quad |x_{\text{NH}_3} - x_{\text{NH}_3}^{\text{aq}}| \leq \varepsilon \quad (16)$$

The mass percent of ammonium bisulfide in the aqueous phase, which is a corrosive environmental parameter to be managed, can be estimated by equation (17).

$$\frac{51.111 \cdot x_{\text{NH}_3}}{17.031 \cdot x_{\text{NH}_3} + 34.082 \cdot x_{\text{H}_2\text{S}} + 18.02 \cdot x_{\text{H}_2\text{O}}} \quad (17)$$

3.3 Dissolution Model in Tube Upper Surface Condensed Aqueous Phase

Solving the dissolution model in the bulk aqueous condensed water explained in the previous section, the ammonia partial pressure in the vapor phase at the bulk liquid temperature T_{Bulk} can be obtained. As mentioned before with Figure 2, in some cases, the tube upper surface temperature T_{Surface} becomes lower than the bulk temperature, and at that time, a surface condensate drop or film at T_{Surface} appears. When NH_3 dissolves there and an equal amount of H_2S dissolves as a neutralization reaction, then the concentration of NH_4HS becomes extremely high from the equilibrium absorption phenomena, and severe corrosion occurs. Therefore, estimating the mass concentration of NH_4HS in the tube upper surface condensed aqueous phase is much important for managing the reliability of the facility during operation. The amount of condensed water as drops or film on the tube upper surface is negligibly small, so that the dissolved NH_3 and H_2S molar fractions ($x_{\text{NH}_3}^{\text{s}}$, $x_{\text{H}_2\text{S}}^{\text{s}}$) in the tube upper surface condensed water can be interpreted as expressed in Eq. (18).

$$x_{\text{NH}_3}^{\text{s}} = x_{\text{H}_2\text{S}}^{\text{s}} = \exp\left(\frac{2061}{T_{\text{Surface}}} - 10.279\right) \cdot p_{\text{NH}_3}^{0.5} - \exp\left(\frac{5556.6}{T_{\text{Surface}}} - 26.793\right) \cdot p_{\text{NH}_3} \quad (18)$$

The mass percent of NH_4HS in the aqueous phase, which is a corrosion environmental parameter to be managed, can be estimated by equation (19).

$$\frac{51.111 \cdot x_{\text{NH}_3}^{\text{S}}}{51.111 \cdot x_{\text{NH}_3}^{\text{S}} + 18.02 \cdot (1 - 2 \cdot x_{\text{NH}_3}^{\text{S}})} \quad (19)$$

4. Three Layers Model for Predicting Corrosion Environmental Condition

Figure 4 shows the corrosion environmental condition prediction layer which describes the hierarchical input/output relations between the above mentioned dissolution models. The pale green boxes represent functional sub-models indicated by equation numbers, and light blue boxes represent internal variables. The pink boxes represent the interface for indicating the NH_4HS corrosion environmental conditions, and the white boxes represent the required input parameters.

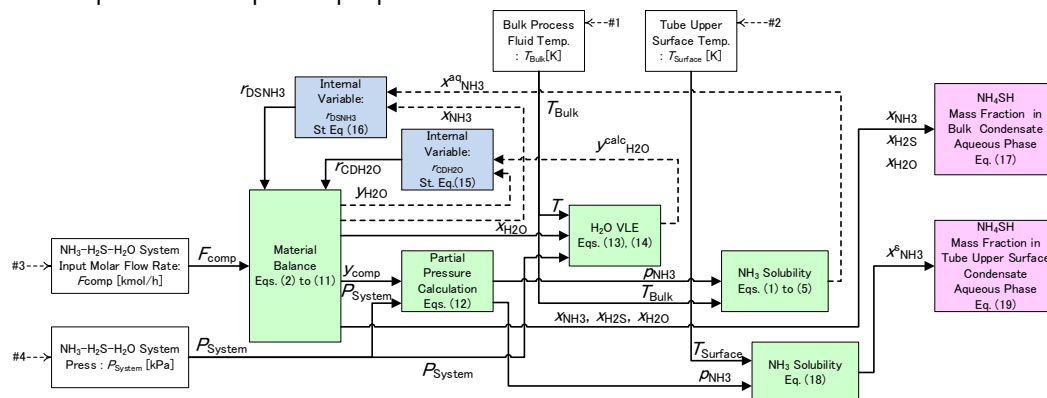


Figure 4 Equilibrium solubility based hierarchical model to predict NH_4HS concentration in aqueous phase

On the other hand, Figure 5 shows process simulation scheme for the process bulk simulation layer correcting the operation data and providing the process parameters which are necessary for the corrosion environmental condition prediction layer. In this scheme, the heat transfer tube of “C-204: Reactor Effluent Condenser” is represented by a series of plural number of decanter unit with cooler. Performing flow sheet simulation, the Peng Robinson thermodynamic model is used, and the necessary process parameters (P_{system} , p_{comp} , F_{comp} and T_{Bulk}) for predicting corrosion environmental conditions can be retrieved from the aqueous liquid and vapour flows of the decanters. Unfortunately, T_{Surface} : tube surface temperature should be estimated from the temperature difference between “C-204” outlet temperature and T_{Air} : ambient one.

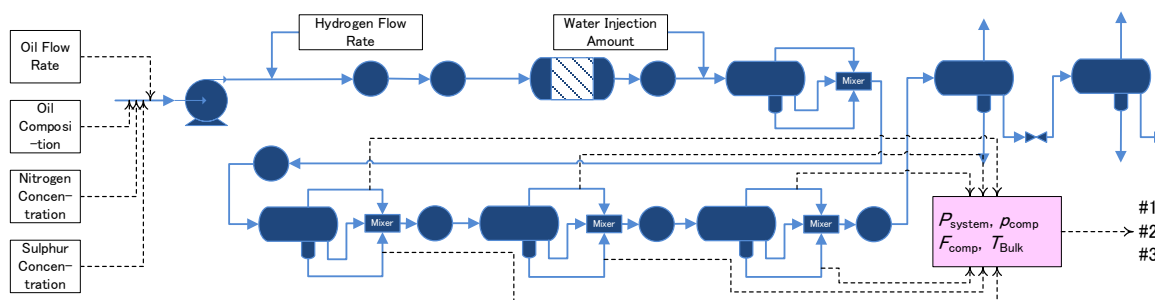


Figure 5 Process simulation scheme for process bulk simulation layer

Furthermore the process bulk simulation layer receives operating conditions including the raw material oil, hydrogen and injected water flow rates, their compositions and the other process parameters of TPFLC (Temperature, Pressure, Flow, Composition) process parameters, from the process information management system, which will be implemented on the upper level than the operating system. The required information may be retrieved via the item number as shown in the flow diagram in Figure 1.

5. Case Study

For the HDS plant shown in Figure 1, a case study is performed using the developed NH_4HS corrosion environmental condition prediction model using design data instead of the normal plant operation data. In this

study, DWSim 6.7.1 (<https://dwsim.fossee.in/>) was used as a process bulk simulator, and an off-line external program was implemented for the corrosion environment condition prediction layer. Table 1 shows the outline of oil, hydrogen and injection water. These are based on the design values, but the physical properties that can be used with the simulator are limited, so that the average molecular weight of the oil components was only adjusted. As shown in Table 2, sulphur and nitrogen components are assumed to be “Thiophene” and “Aniline”. Changes in the corrosion environment were investigated when the feedstock oil was changed from the current operating conditions of 1.8 wt% sulfur and 150 wt ppm nitrogen to 350 wt ppm nitrogen as shown in Figure 6. Where, the temperature difference between the bulk fluid and tube upper surface is assumed to be 40 K.

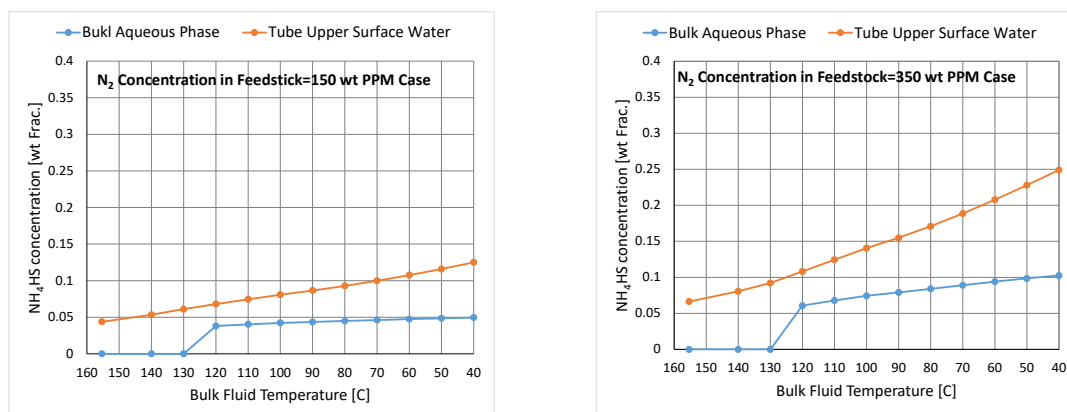


Figure 6 Comparison of corrosion environments with different concentrations of N₂ in feedstock

Table 1: Oil, gas, injected water condition for design basis

	Feed Oil	Make up Gas	Recycle Gas	Injected Water
Flow Rate (kg/h)	91,100	1,402	5,579	912
MW	250.0	4.80	6.80	18.02
Temperature (C)	138	40	64	43
Pressure (MPa)	7,823	8,927	7,810	6,810
S (wt%)	1.8			
N (wt ppm)	150	-	-	-

6. Conclusions

The purpose of this research is to predict how changes, such as changing raw materials, which are performed by the operation to increase productivity and reduce cost, will affect the deterioration of plant assets, and to conduct production planning in consideration of asset management. And a system for enabling a maintenance plan to be made consistent with the production plan. Insufficient change management has been pointed out as the cause of many incidents, and the realization of this corrosion environmental condition prediction directly leads to a reduction in incidents due to inconsistencies between operation and equipment conditions, and contribute to the sustainable of the chemical industry.

Acknowledgments

The authors are grateful to the following plant maintenance experts for their cooperation; Mr. Iuchi, Kensuke (Safety Case Research Lab.), Mr. Hosoda, Kazutaka (Fuji Oil), Mr. Kumazawa, Nobumitsu (Kumazawa Consultant Office), Mr. Shigekuni, Eiji (Tokuyama), Mr. Shinohara, Hitoshi (Tokuyama), Mr. Tsuyoshi Takehara (NUC)..

References

- Scherrer, C., M. Durrieu, and G. Jarno (1980). Distillate and residue hydroprocessing coping with corrosion with high concentration of ammonium bisulfide in the process water. *Material Performance* 19, 11-25.
- Sherwood, T. K. (1925). Solubilities of Sulfur Dioxide and Ammonia in Water, *Ind. Eng. Chem* 17, 745-747.
- Toba, K. (2013). Application of Simulation Technique on Studies of Ammonium Salts Corrosion in Oil Refining Plants, *Zairyo-to-Kankyo* 62, 352-358 (Japanese).